Two-Dimensional Imaging of O2, H2O2, and Glucose Distributions by an Array of 400 Individually Addressable Microelectrodes

ARTICLE *in* ANALYTICAL CHEMISTRY · APRIL 1995

Impact Factor: 5.64 · DOI: 10.1021/ac00103a005

8 AUTHORS, INCLUDING:

Bernd Gründig
SensLab GmbH
39 PUBLICATIONS **925** CITATIONS
SEE PROFILE

Karl Cammann
University of Münster
365 PUBLICATIONS **3,615** CITATIONS
SEE PROFILE

Anal. Chem. **1995,** *67,* 1164−1170

Two-Dimensional Imaging of O_2, H_2O_2, and Glucose Distributions by an Array of 400 Individually Addressable Microelectrodes

Heinrich Meyer,* Heinz Drewer, Bernd Gründig, and Karl Cammann

Institut für Chemo- und Biosensorik e. V. Mendelstrasse 7, and Lehrstuhl für Analytische Chemie, Westfälische Wilhelms-Universität Münster, Wilhelm-Klemm-Strasse 8, D-48149 Münster, Germany

Ralf Kakerow, Yiannos Manoli, Wilfried Mokwa, and Matthias Rospert

Fraunhofer-Institut für Mikroelektronische Schaltungen und Systeme, Finkenstrasse 61, D-47057 Duisburg, Germany

A monolithic array of 400 individually addressable microelectrodes was fabricated in a modified CMOS process. The platinum electrodes, each 36 μm × 36 μm in size, were arranged in a square matrix of overall area 1 cm². Individual addressing of each electrode in the array was realized by two on-chip shift registers coupled with array control logic. In the electrochemical scanning mode, the 400 electrode signals were read successively. The array was used in supporting electrolyte solutions for imaging of oxygen distributions detected amperometrically at −0.8 V vs Ag/AgCl. Hydrogen peroxide and glucose distributions were imaged amperometrically at +0.8 V vs Ag/AgCl. Prior to imaging glucose distributions, the enzyme glucose oxidase was entrapped into the conducting polymer polypyrrole simultaneously on all array electrodes. Two minutes was needed for a successive readout of all 400 microelectrode signals. Diffusion of the analytes was imaged in a time-resolved manner by a sequence of successive scans. Therefore, the array of individually addressable microelectrodes can be regarded as an alternative electrochemical imaging device to the scanning electrochemical microscope.

Since Clark and Lyons invented the amperometric glucose electrode in 1962,[1] materials as well as technologies for the fabrication of chemical and biochemical sensors[2−6] have changed enormously. Nowadays, the use of thin-film transducers instead of macroelectrodes is very popular because of their miniature size and the possibility of mass production.[7,8] Thin-film technology is characterized by a very high precision in the fabrication process and is therefore an ideal technology for fabricating arrays of electrodes with small electrode diameters and interelectrode distances.[9] Such microelectrode arrays must be categorized into two different types: arrays with parallel connected microelectrodes and arrays with individually addressable microelectrodes.[10] The first type of array has been investigated very intensively due to its special features.[11−19] Until now, two-dimensional arrays of individually addressable microelectrodes have been produced very rarely, mainly due to their sophisticated demands on technology and electronic circuitry. There are two different ways of realizing individual addressing of array electrodes: each electrode may be connected by its own line to a corresponding bond pad on the chip border.[20,21] This way of realization is quite easy from a technological view point, but there is a limit to the number of individually addressable microelectrodes which is determined by the space on the chip border available for bond pads. Alternatively, individual addressing of array electrodes can be realized on chip by an integrated circuit (IC). Recently, we presented such an array for the first time and described the technological process of chip production and the layout of the monolithic microelectrode array in detail.[22,23] Moreover, results obtained for the potentiometric imaging of distributions of ammonium chloride and of urea have been published.[24] In this paper, we present results for the

(1) Clark, L. C., Jr.; Lyons, C. *Ann. N.Y. Acad. Sci.* **1962**, *102*, 29−45.
(2) Turner, A. P. F., Karube, I., Wilson, G. S., Eds.; *Biosensors—Fundamentals and Applications*; Oxford University Press, Oxford, U.K., 1987.
(3) Collowick, S., Kaplan, N. O., Mosbach, K., Eds.; *Methods in Enzymology*; Academic Press: San Diego, CA, 1988; Vol. 137.
(4) Scheller, F.; Schubert, F. *Biosensors, Techniques and Instrumentation in Analytical Chemistry*; Elsevier: Amsterdam, 1992; Vol. 11.
(5) Wagner, G., Guilbault, G. G., Eds.; *Food Biosensor Analysis*; Marcel Dekker: New York, 1994.
(6) Cammann, K.; Roβ, B.; Hasse, W.; Dumschat, C.; Katerkamp, A.; Reinbold, J.; Steinhage, G.; Gründig, B.; Renneberg, R.; Buschmann, N. In *Ullmann's Encyclopedia of Industrial Chemistry*; VCH: Weinheim, Germany, 1994; Vol. B6 pp 121−212.
(7) Hughes, R. C.; Ricco, A. J.; Butler, M. A.; Martin, S. J. *Science* **1991**, *254*, 74−80.
(8) Alvarez-Icaza, M.; Bilitewski, U. *Anal. Chem.* **1993**, *65*, 525A−533A.
(9) Wu, Q.; Lee, K.-M.; Liu, C.-C. *Sens. Actuators* **1993**, *B13−14*, 1−6.
(10) Diamond, D. *Electroanalysis* **1993**, *5*, 795−802.
(11) Gueshi, T.; Tokuda, K.; Matsuda, H. *J. Electroanal. Chem.* **1978**, *89*, 247−260.
(12) Shoup, D.; Szabo, A. *J. Electroanal. Chem.* **1984**, *160*, 19−26.
(13) Thormann, W.; van den Bosch, P.; Bond, A. M. *Anal. Chem.* **1985**, *57*, 2764−2770.
(14) Cassidy, J.; Ghoroghchian, J.; Sarfarazi, F.; Smith, J. J.; Pons, S. *Electrochim. Acta* **1986**, *31*, 629−636.
(15) Hepel, T.; Osteryoung, J. *J. Electrochem. Soc.* **1986**, *133*, 752−757.
(16) Scharifker, B. R. *J. Electroanal. Chem.* **1988**, *240*, 61−76.
(17) Tallman, D. E.; Petersen, S. L. *Electroanalysis* **1990**, *2*, 499−510.
(18) Roβ, B.; Cammann, K.; Mokwa, W.; Rospert, M. *Sens. Actuators* **1992**, *B7*, 758−762.
(19) Kolev, S. D.; Simons, J. H. M.; van der Linden, W. E. *Anal. Chim. Acta* **1993**, *273*, 71−80.
(20) Dees, D. W.; Tobias, C. W. *J. Electrochem. Soc.* **1987**, *134*, 369−377.
(21) Connolly, P.; Moores, G. R.; Monaghan, W.; Shen, J.; Britland, S.; Clark, P. *Sens. Actuators* **1992**, *B6*, 113−121.
(22) Kakerow, R.; Manoli, Y.; Mokwa, W.; Rospert, M.; Cammann, K.; Krause, J.; Meyer, H. *Technical Digest, Transducers '93*, Yokohama, Japan, June 7−10, 1993; pp 1074−1077
(23) Kakerow, R.; Manoli, Y.; Mokwa, W.; Rospert, M.; Meyer, H.; Drewer, H.; Krause, J.; Cammann, K. *Sens. Actuators* **1994**, *A43*, 296−301.

0003-2700/95/0367-1164$9.00/0

amperometric imaging of O_2 and H_2O_2 distributions as well as glucose distributions after immobilization of glucose oxidase (GOx) onto the array electrodes.

Fiaccabrino et al.[25] have also reported the fabrication of a monolithic microelectrode array. In their work, the use of an IC for the individual addressing of 100 platinum microelectrodes was demonstrated in principle. Compared with the scanning electrochemical microscopy (SECM),[26–30] the array approach of electrochemical imaging offers new possibilities: first, the imaging of diffusion processes is no longer disturbed by a tip that is moved across the substrate. Second, the microelectrode array may be provided with long addressing lines. Thus, a freely movable electrochemical imaging device is available which may be put onto or even into the object of investigation. In SECM, the substrate has to be prepared especially for the analyzing instrument and, thereafter, has to be carried into a small electrolyte vessel before starting the experiment. Normally, this may not be a problem, even if biological probes are investigated.[31,32] However, this is impossible whenever large living objects such as human organs are investigated or when on-line analysis is necessary, e.g., in tubes of process apparatus, where the screening of local corrosion processes is very important.

EXPERIMENTAL SECTION

Array of 400 Individually Addressable Microelectrodes. The microelectrode array was fabricated as a part of a monolithic sensor chip in a modified complementary metal oxide semiconductor (CMOS) process. For details concerning the chip layout and its fabrication see Kakerow et al.[23]

The 400 individually addressable microelectrodes are arranged in a square matrix of 20 × 20 sensor cells. The size of one single sensor cell is 500 μm × 500 μm. Each sensor cell contains one 36 μm × 36 μm platinum microelectrode, a readout amplifier, and a sensor cell control unit. The readout amplifier converts the electrode potential to an analog output current. It is activated only when the sensor array is used in test mode or potentiometric mode and has not been used for the results presented here. Switching between test mode, potentiometric mode, and amperometric mode is performed by the sensor cell control unit.

Individual addressing of each sensor cell is realized by two on-chip shift registers and sensor array control logic. Thus, scanning of the complete array can be performed by reading the 400 individual sensor signals successively.

Apparatus. The experimental setup used for voltammetric and amperometric measurements is shown in Figure 1. The sensor array was controlled by an IBM-compatible 486DX 33 MHz personal computer via a digital I/O card with a standard controller chip (type 8255), whereas the potentiostat was controlled via an IEEE 488.2 card from National Instruments (Austin, TX). The

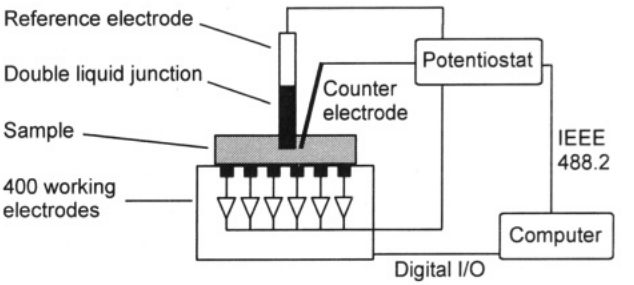

Figure 1. Experimental setup for amperometric and voltammetric measurements.

software used for operational control and reading of the analog output data was developed in-house. A HM 8040 from Hameg (Frankfurt, Germany) was used as the chip power supply (not depicted). The supplied voltage was ±5 V. The potentiostat was a PAR 273 model from EG&G (München, Germany). A Ag/AgCl/3 M KCl electrode with double liquid junction was used as an external reference, and a platinum foil was used as an external counter electrode (both from Metrohm, Filderstadt, Germany).

Electrolyte solutions were stirred by an IKAMAG REO S4 magnetic stirrer from IKA-Labortechnik (Staufen, Germany). For calibration of the microelectrode array with oxygen, defined oxygen to nitrogen ratios were adjusted by a gas mixture apparatus fabricated in our laboratory.

Reagents. All reagents were purchased from Sigma (Deisenhofen, Germany) and were of the highest available grade. Oxygen (99.995%) and nitrogen (99.998%) gases were purchased from Westfalen Gas (Münster, Germany). The reagents were used as received. Only pyrrole was purified by distillation under nitrogen before use. Glucose solutions were allowed to mutarotate overnight before use. Glucose oxidase (EC 1.1.3.4) was from *Aspergillus niger* (Sigma VII S) with a certified activity of 150.000 units/g.

Procedures. *Cyclic Voltammetry (CV).* CV was used for cleaning the array electrodes. Therefore, the potential was cycled in the supporting electrolyte solution between −0.8 and +1.2 V vs Ag/AgCl, until the voltammogram showed no further changes. This cleaning procedure was performed simultaneously for all 400 array electrodes each time before starting a new experiment.

CV was also used for characterizing the sputtered platinum microelectrodes. Therefore, the chip was completely immersed in an unstirred solution of 5 mM $[Ru(NH_3)_6]Cl_2$ and 5 mM $[Ru(NH_3)_6]Cl_3$ in 0.1 M nitrogen-saturated potassium chloride. A solution of 0.1 M KCl was used as supporting electrolyte for determining the voltammetric oxygen wave, and a solution of 0.05 M phosphate buffer (pH 7.0) was used for determining the voltammetric hydrogen peroxide wave.

Amperometric Scanning Procedure. During an amperometric scan, the steady-state currents of 400 array electrodes have to be maintained as well as possible while reading of the individual electrode signals occurs successively using the same analog output line. Therefore, a sensor array control logic was created. Some terms typically used in IC technology are introduced in Figure 2.

DCLOCK (±5 V) represents the frequency for switching from sensor cell to sensor cell. Once started by a digital control signal DRESET, each new clock phase automatically switches to the next sensor cell. DCLOCK is generated by the computer and its frequency can be varied by the software. The potentiostat is

(24) Meyer, H.; Drewer, H.; Krause, J.; Cammann, K.; Kakerow, R.; Manoli, Y.; Mokwa, W.; Rospert, M. *Sens. Actuators* **1994**, *B18*, 229–234.
(25) Fiaccabrino, G. C.; Koudelka-Hep, M.; Jeanneret, S.; van den Berg, A.; de Rooij, N. F. *Sens. Actuators* **1994**, *B19*, 675–677.
(26) Bard, A. J.; Fan, F.-R. F.; Kwak, J.; Lev, O. *Anal. Chem.* **1989**, *61*, 132–138.
(27) Kwak, J.; Bard, A. J. *Anal. Chem.* **1989**, *61*, 1221–1227.
(28) Kwak, J.; Bard, A. J. *Anal. Chem.* **1989**, *61*, 1794–1799.
(29) Engstrom, R. C.; Pharr, C. M. *Anal. Chem.* **1989**, *61*, 1099A–1104A.
(30) Bard, A. J.; Denuault, G.; Lee, C.; Mandler, D.; Wipf, D. O. *Acc. Chem. Res.* **1990**, *23*, 357–363.
(31) Scott, E. R.; White, H. S.; Phipps, J. B. *Anal. Chem.* **1993**, *65*, 1537–1545.
(32) Pierce, D. T.; Bard, A. J. *Anal. Chem.* **1993**, *65*, 3598–3604.

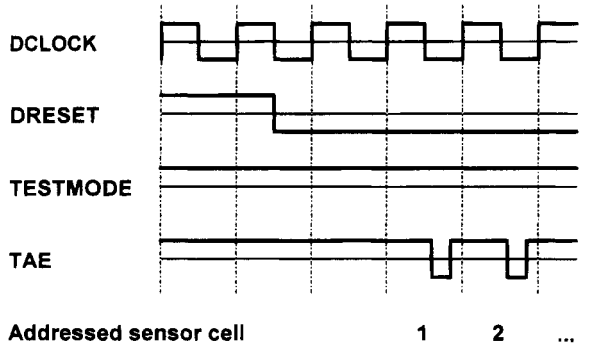

Figure 2. Control logic for the amperometric scanning mode.

connected to the chip via an input line. When the control signal TESTMODE is set on "high" (+5 V) and TAE is set on "low" (−5 V), only the actually addressed sensor cell is connected to the potentiostat. When TAE is set on "high", all 400 sensor cells are connected simultaneously to the potentiostat.

For an amperometric scan, all electrodes first have to establish their steady-state currents. Therefore, TAE is set on "high" for an adjustable preconditioning time period, while TESTMODE is also on "high". DRESET starts the scan with a scan rate according to the preselected DCLOCK frequency. At the end of each DCLOCK phase, TAE is set on "low" for a short readout time period, in which only the addressed electrode is connected to the potentiostat. After reading out the individual sensor signal, TAE is set back on "high" to reestablish the 400 steady-state currents. Thereafter, a new DCLOCK phase switches to the next sensor cell. The switching of TAE occurs 400 times during each amperometric scan. For the results presented here, we chose a preconditioning time (TAE high) of 60 s prior to starting the amperometric scan, a DCLOCK phase time of 300 ms, and a readout time (TAE low) of 150 ms.

Amperometric Calibration Procedure. For sensor array calibration, the chip was dipped into 40 mL of the corresponding electrolyte solution. Calibration with oxygen was performed by purging a 0.1 M KCl solution with the appropriate oxygen/nitrogen gas mixtures for at least 10 min. Then, purging was stopped and the amperometric scan was started at −0.8 V vs Ag/AgCl. During the scan, the gas mixture was continuously passed over the electrolyte solution. Calibration with hydrogen peroxide or glucose, respectively, was performed by adding corresponding stock solutions to a 0.05 M phosphate buffer solution (pH 7.0) which was stirred continuously at 300 rpm. The applied potential was +0.8 V vs Ag/AgCl.

Amperometric Imaging Procedure. For imaging experiments, the chip was arranged in a horizontal position according to Figure 1. The sensor array was always covered with 400 μL of the relevant supporting electrolyte solution: 0.1 M KCl for imaging of oxygen distributions and 0.05 M phosphate buffer solution (pH 7.0) for imaging of hydrogen peroxide or glucose distributions, respectively. An analyte solution was filled into the double liquid junction, which had a frit diameter of 2 mm. After contact of the double liquid junction to the electrolyte solution on the chip, the analyte streamed out of the double liquid junction through the frit and into the electrolyte solution on the chip. This streaming out of the analyte and its subsequent distribution all over the sensor array was imaged by successive amperometric scans. For imaging of oxygen, the double liquid junction was filled with a solution of 1 M sodium sulfite in 0.1 M KCl. Sodium sulfite reduced oxygen by forming sodium sulfate. This reduction was imaged at an working potential of −0.8 V vs Ag/AgCl. For imaging of hydrogen peroxide or glucose, respectively, the double liquid junction was filled with 1 M hydrogen peroxide or glucose in 0.05 M phosphate buffer (7.0). Successive amperometric scans were performed at +0.8 V vs Ag/AgCl.

Enzyme Immobilization Procedure. GOx was immobilized onto the array electrodes via electrochemical entrapment into the conducting polymer polypyrrole according to the following procedure:[33-39] the monolithic chip was dipped into 40 mL of an unstirred, deaerated solution of 0.1 M pyrrole, 1000 units/mL GOx, and 0.1 M KCl in 0.05 M phosphate buffer (pH 7.0). Polypyrrole was electropolymerized on top of all 400 platinum microelectrodes simultaneously by applying a constant working potential of +0.8 V vs Ag/AgCl for 5 min. Thereafter, the chip was washed several times with phosphate buffer solution (pH 7.0). When the chip was not in use, it was stored in the same buffer solution at room temperature.

RESULTS AND DISCUSSION

Microelectrode Array Characterization by Cyclic Voltammetry. For characterizing the sputtered platinum array electrodes, cyclic voltammetry was carried out in a solution of 5 mM $[Ru(NH_3)_6]Cl_2/[Ru(NH_3)_6]Cl_3$ in 0.1 M KCl. Figure 3 shows cyclic voltammograms from +0.2 V to −0.5 V vs Ag/AgCl with a scan rate of 100 mV/s. For the cyclic voltammogram in Figure 3a) only one individual array electrode was addressed, whereas for the cyclic voltammogram in Figure 3b) all 400 array electrodes were addressed simultaneously.

A sigmoidally shaped voltammogram instead of a peak-shaped one is typical for a microelectrode.[40-43] Thus, these cyclic voltammograms clearly characterize the array electrodes as microelectrodes. Moreover, Figure 3 demonstrates that the current density did not significantly depend on whether only an individual array electrode was addressed (Figure 3a) or all 400 array electrodes were addressed (Figure 3b). From this we concluded that the diffusion layers of the 400 array electrodes did not overlap here and that we were allowed to regard the 400 individual electrode signals as 400 independent current signals at short or intermediate time scales.[14,16]

Oxygen Measurements. In Figure 4, cyclic voltammograms from +0.1 to −0.9 V vs Ag/AgCl (only the forward scans are depicted for clarity) indicate that the sputtered platinum electrodes could be used for oxygen detection at cathodic potentials as low as −0.8 V vs Ag/AgCl. At more negative potentials, the current increased due to hydrogen evolution.

(33) Umana, M.; Waller, J. *Anal. Chem.* **1986**, *58*, 2979–2983.
(34) Foulds, N. C.; Lowe, C. R. *J. Chem. Soc., Faraday Trans. 1* **1986**, *82*, 1259–1264.
(35) Bartlett, P. N.; Whitaker, R. G. *J. Electroanal. Chem.* **1987**, *224*, 37–48.
(36) Bélanger, D.; Nadreau, J.; Fortier, G. *J. Electroanal. Chem.* **1989**, *274*, 143–155.
(37) Yon Hin, B. F. Y.; Sethi, R. S.; Lowe, C. R. *Sens. Actuators* **1990**, *B1*, 550–554.
(38) Fortier, G.; Bélanger, D. *Biotechnol. Bioeng.* **1991**, *37*, 854–858.
(39) Strike, D. J.; Arquint, P.; de Rooij, N. F.; Koudelka-Hep, M. *Chimia* **1993**, *47*, 241–244.
(40) Wightman, R. M. *Anal. Chem.* **1981**, *53*, 1125A–1134A.
(41) Aoki, K.; Akimoto, K.; Tokuda, K.; Matsuda, H.; Osteryoung, J. *J. Electroanal. Chem.* **1984**, *171*, 219–230.
(42) Fleischmann, M., Pons, S., Rolison, D. R., Schmidt, P. P., Eds.; *Ultramicroelectrodes*; Datatech Systems Publishers: Morganton, NC, 1987.
(43) Bond, A. M.; Oldham, K. B.; Zoski, C. G. *Anal. Chim. Acta* **1989**, *216*, 177–230.

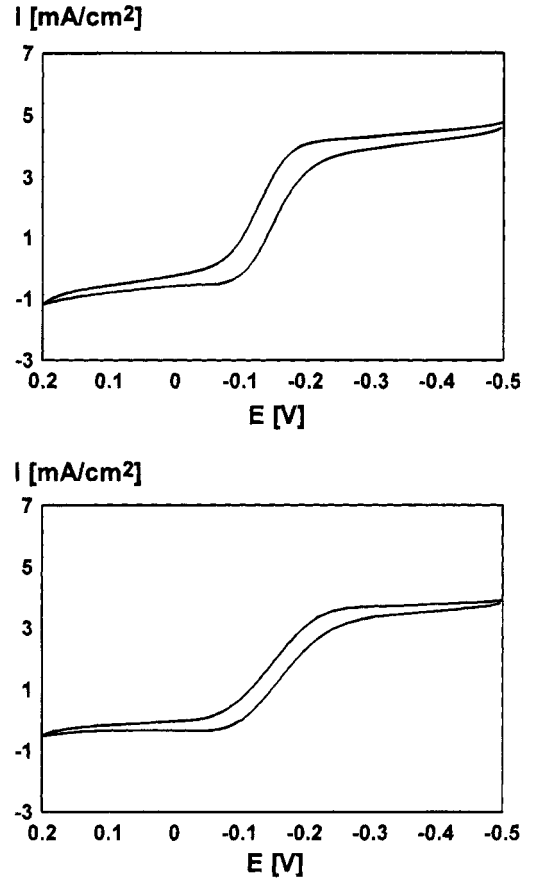

Figure 3. Cyclic voltammograms in 5 mM $[Ru(NH_3)_6]Cl_2/[Ru(NH_3)_6]Cl_3$ (in 0.1 M KCl) for (a, top) an individual platinum microelectrode and (b, bottom) all 400 microelectrodes simultaneously. Scan rate 100 mV/s.

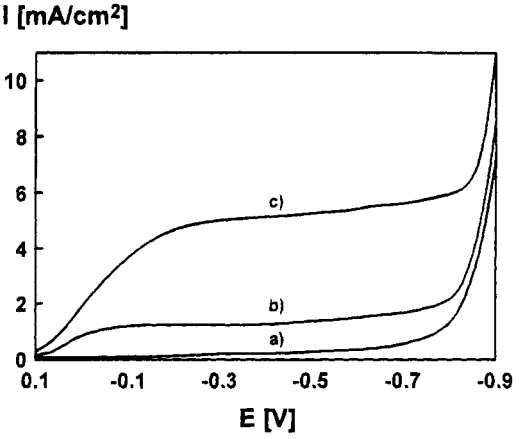

Figure 4. Cyclic voltammogram (forward scan) of a platinum microelectrode in (a) nitrogen-, (b) air-, and (c) oxygen-saturated 0.1 M KCl. Scan rate 100 mV/s.

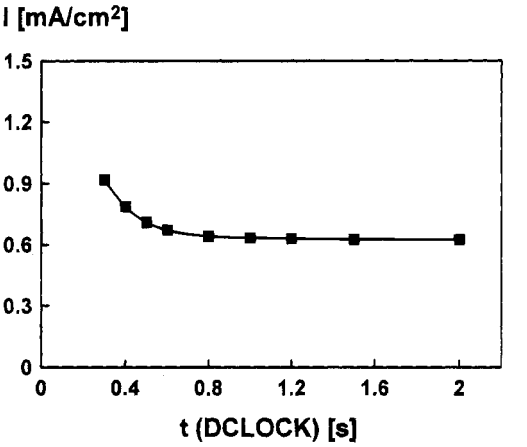

Figure 5. Amperometric reduction of oxygen in air-saturated 0.1 M KCl at −0.8 V vs Ag/AgCl. Preconditioning time 60 s; readout time 150 ms.

The amperometric measurement of oxygen at −0.8 V vs Ag/AgCl in air-saturated 0.1 M KCl was used to demonstrate the correlation between the electrode signals and the scan time selected for the amperometric scan. Therefore, the preconditioning time and the DCLOCK phase time and readout time within the DCLOCK phase were varied. As a result, we obtained a minimum readout time of 0.15 s. At shorter times we obtained scattered signals without a clear trend including negative instead of positive currents. The minimum preconditioning time was approximately 60 s (t_{95}). The relation between the DCLOCK phase time and the corresponding electrode signals in the amperometric scanning mode is shown in Figure 5.

Each point of this graph represents the mean of 400 individual electrode signals from a complete amperometric scan. The figure can be interpreted as follows: whenever an individual electrode signal was read during the readout time, all other electrodes were disconnected from the potentiostat by the sensor cell control units. For that time period, these electrodes were in open circuit. After reading the individual electrode signal, the other electrodes were reconnected to the potentiostat. Then, reconditioning, i.e., reestablishment of the steady-state current at all electrodes, occurred each time. When the time period for reconditioning was short, for example, for DCLOCK phase times of less than 1 s, reading of the electrode signals started before the corresponding steady-state currents had been reestablished. As can be seen from Figure 5, DCLOCK phase times of 1 s or more allowed complete achievement of the steady-state currents during the reconditioning time. The corresponding standard deviation ($n = 400$) decreased from 5.8% for 0.3 s and 1.0% for 1.0 s to 0.6% for a 2.0 s DCLOCK phase time. Therefore, if accurate measurements are desired, long DCLOCK phase times are necessary. However, if short scan times are desired, for example, in time-resolved imaging experiments, less accurate data will have to be accepted.

In order to achieve scan times as short as possible, a DCLOCK phase time of 0.3 s was selected in all the following experiments accepting the corresponding decrease in accuracy.

Based on amperometric detection at −0.8 V vs Ag/AgCl, an oxygen calibration was performed in 0.1 M KCl using the amperometric scanning mode. The corresponding calibration graph was linear from 0 to 100% oxygen saturation. The sensitivity was 40.7 ± 0.4 $\mu A/cm^2$ per percent oxygen saturation or 40.2 ± 0.4 nA/cm^2 per Pa oxygen partial pressure (pO_2), respectively ($n = 12$). The mean current density in nitrogen-saturated solution was 40 $\mu A/cm^2$ with a standard deviation of 20 $\mu A/cm^2$.

For comparison, a second oxygen calibration was carried out using a single platinum disk electrode (diameter 0.5 mm). On applying the same conditions to the macroelectrode, a sensitivity of 7.3 ± 0.3 $\mu A/cm^2$ per percent O_2 or 7.2 ± 0.3 nA/cm^2 per Pa pO_2, respectively, was obtained ($n = 6$). Thus, the sensitivity of the array electrodes was larger than the sensitvity of the macroelectrode by a factor of 5.6. This indicated at least a partial hemispherical instead of planar diffusion of oxygen to the surface of the array electrodes.[14,16]

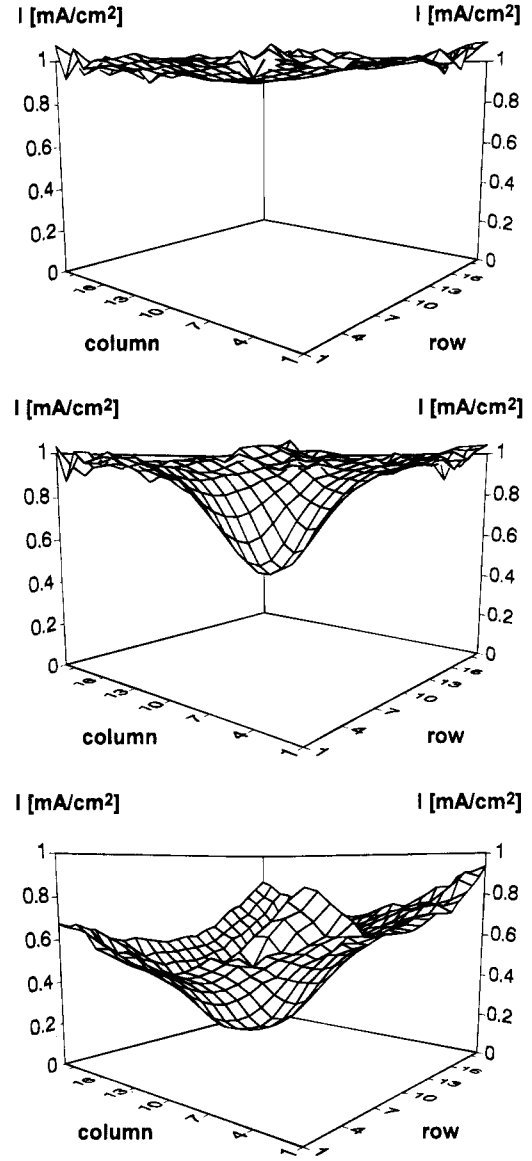

Figure 6. Imaging of oxygen reduction by sodium sulfite in 0.1 M KCl at −0.8 V vs Ag/AgCl. Scan time 2 min. Scans started after (a, top) 3, (b, middle) 13, and (c, bottom) 23 min.

The imaging of oxygen reduction by sodium sulfite streaming into air-saturated 0.1 M KCl is depicted in Figure 6a–c.

This sequence of three amperometric scans, each of scan time 2 min and started 3 (a), 13 (b), and 23 min (c) after the contact of the double liquid junction to the supporting electrolyte solution on the chip (see imaging procedure), shows that sodium sulfite streamed continuously out of the double liquid junction into the electrolyte solution covering the chip. There, it reduced dissolved oxygen by formation of sodium sulfate. Consequently, the concentration of dissolved oxygen decreased. In Figure 6a–c, a decrease in current signal corresponds to a decrease in oxygen concentration. Due to the arrangement of the double liquid junction at the center of the microelectrode array in close proximity to the array electrodes, oxygen reduction was indicated there first (Figure 6b). Thereafter, the sodium sulfite diffused laterally, resulting in oxygen reduction all over the microelectrode array (Figure 6c). After 63 min, oxygen was no longer detectable at the center of the array, but at the array edges all electrode signals were still in the range of 0.2–0.3 mA/cm^2 (not depicted). Thus, it may be concluded that after hours no oxygen would have been detectable anywhere on the microelectrode array. Therefore, Figure 6 clearly demonstrates that the microelectrode array reported in this study can be used for time-resolved amperometric imaging of processes that are in the time scale of minutes or longer.

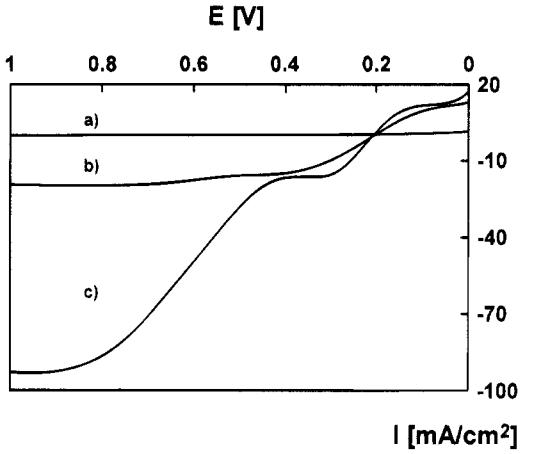

Figure 7. Cyclic voltammogram (forward scan) of a platinum microelectrode in 0.05 M phosphate buffer (pH 7.0) (a) without H_2O_2, (b) with 0.01 M H_2O_2, and (c) with 0.05 M H_2O_2. Scan rate 100 mV/s.

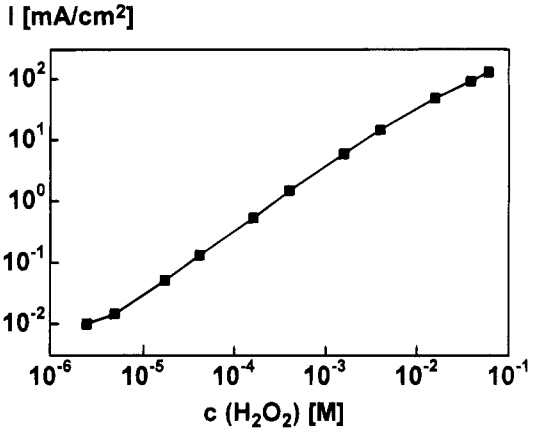

Figure 8. Calibration graph for H_2O_2 in 0.05 M phosphate buffer (pH 7.0) at +0.8 V vs Ag/AgCl.

Hydrogen Peroxide Measurements. Cyclic voltammetry was performed with an individual platinum array electrode in 0.05 M phosphate buffer (pH 7.0) containing different amounts of hydrogen peroxide (Figure 7). For clarity, only the forward scans are depicted here. They show an increase in the anodic current in two consecutive steps. The first step was assigned to the formation of platinum oxides or hydroxides on the surface of the platinum microelectrode. Hydrogen peroxide worked here as a catalyst for the platinum oxidation, because no platinum oxidation peak is present in the background scan. The second step starting at +0.4 V vs Ag/AgCl was generated by the anodic oxidation of hydrogen peroxide.

The corresponding calibration graph for H_2O_2 detection at +0.8 V vs Ag/AgCl is presented in Figure 8. Each point of this calibration graph represents the mean of 400 individual sensor signals of one amperometric scan. The corresponding standard deviations were approximately ±10%. A linear range was obtained from 5×10^{-6} to 5×10^{-3} M with a sensitivity of 3.62 ± 0.01 mA/cm^2 mM^{-1} ($n = 7$). A hydrogen peroxide calibration using a platinum macroelectrode (diameter 0.5 mm) resulted in a graph with a linearity from 5×10^{-6} to 1×10^{-2} M and a sensitivity of

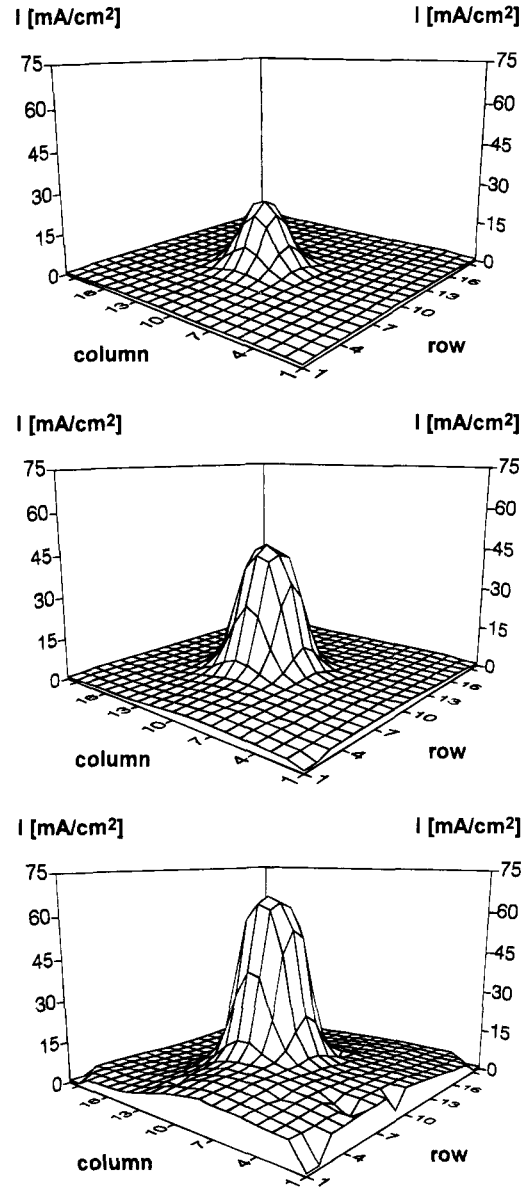

Figure 9. Imaging of H_2O_2 distributions in 0.05 M phosphate buffer (pH 7.0) at +0.8 V vs Ag/AgCl. Scan time 2 min. Scans started after (a, top) 13, (b, middle) 20, and (c, bottom) 27 min.

0.71 ± 0.01 mA/cm^2 mM^{-1} (n = 7). Due to hemispherical diffusion at microelectrodes, the array electrodes are more sensitive to hydrogen peroxide than the macroelectrode by a factor of 5.1.

For imaging of hydrogen peroxide distributions, a solution of hydrogen peroxide was allowed to stream out of the double liquid junction into a phosphate buffer solution on the chip (see imaging procedure). In Figure 9a–c, three scans started 13 (a), 20 (b), and 27 min (c) after contact of the double liquid junction with the phosphate buffer solution on the chip are presented. An increase in current signal indicates an increase in hydrogen peroxide concentration. Again, the analyte was detected first at the center of the electrode array due to the centered arrangement of the double liquid junction (Figure 9a). The H_2O_2 signal increased, but in contrast to oxygen reduction, the changes were observed only in the center region over a period of minutes (Figure 9b). Thereafter, a significant increase in the current signal was also observed in the outer regions (Figure 9c).

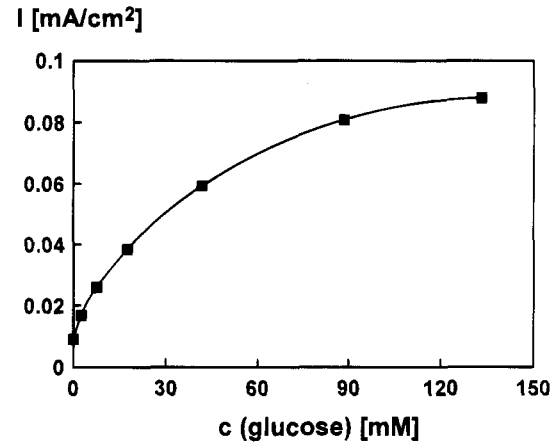

Figure 10. Calibration graph for glucose in 0.05 M phosphate buffer (pH 7.0) at +0.8 V vs Ag/AgCl.

Moreover, in Figure 9c, there are some individual electrode signals which indicate a breakdown of the corresponding anodic current. This was only observed for the detection of high concentrations of H_2O_2 and was caused by adsorbed oxygen gas which, after being produced by anodic oxidation of H_2O_2, blocked the electrode surface.

Glucose Measurements. On the basis of the amperometric measurement of oxygen or hydrogen peroxide, respectively, the monolithic microelectrode array could be used as transducer for oxidases.[44,45] A calibration graph for an enzyme-based measurement of glucose is presented in Figure 10. GOx was immobilized on top of the array electrodes by entrapment into electropolymerized polypyrrole and converted glucose into gluconolactone with the concomitant formation of hydrogen peroxide. Hydrogen peroxide thus produced was detected amperometrically at +0.8 V vs Ag/AgCl and was correlated to the corresponding glucose concentration.

Each point of the calibration graph in Figure 10 represents the mean of 400 single sensor signals. The corresponding standard deviations were approximately ±10%. The limit of detection was 0.5 mM glucose. The response saturated at high glucose concentrations (90 mM). An identical curve was obtained for the platinum macroelectrode. However, this time, the macroelectrode was not significantly less sensitive to glucose than the array electrodes. After modification of the array electrodes by glucose oxidase entrapment into polypyrrole, the enzyme membrane thus formed became diffusion limiting. Hemispherical diffusion was no longer present, and consequently, current densities did not significantly differ from those of the macroelectrode.

Figure 11 shows three amperometric scans started 13 (a), 20 (b), and 27 min (c) after a solution of 1 M glucose was allowed to stream out of the double liquid junction through the frit into the phosphate buffer solution on the chip (see imaging procedure). By measurement of the enzymatic formation of hydrogen peroxide, Figure 11a–c show a continous increase in glucose concentration on the array starting again from the center of the enzyme-modified sensor array. In a manner similar to the diffusion of sodium sulfite in Figure 6, glucose spread symmetrically from

(44) *Enyme Nomenclature 1992—Recommendations of the Nomenclature Committee of the International Union of Biochemistry and Molecular Biology*; Academic Press: San Diego, CA, 1992.

(45) Dixon, M.; Webb, E. C. *Enzymes*; Academic Press, New York, 1979.

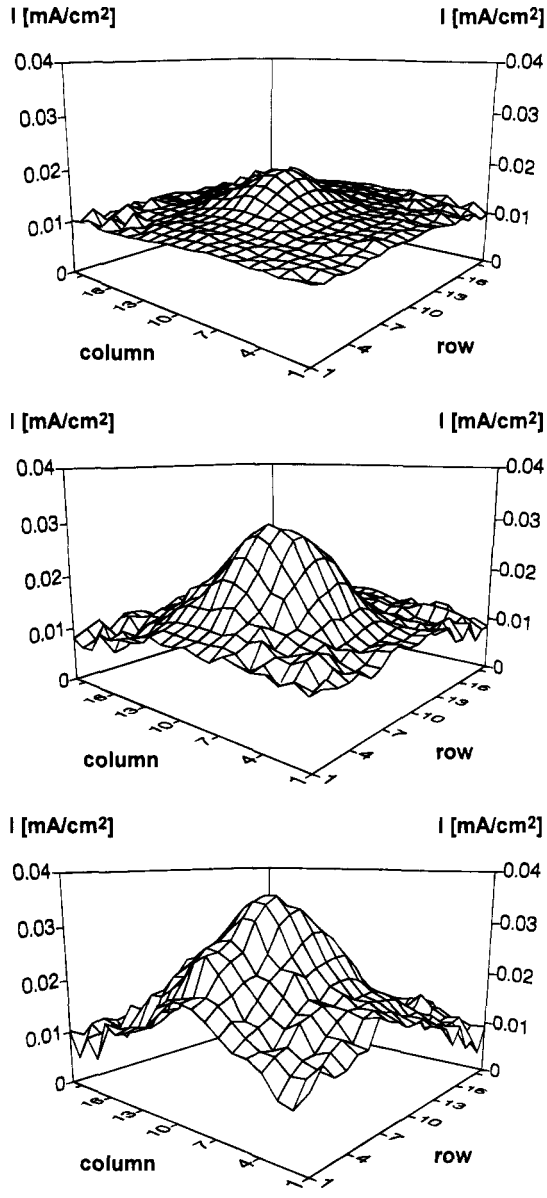

Figure 11. Imaging of glucose distributions in 0.05 M phosphate buffer (pH 7.0) at +0.8 V vs Ag/AgCl. Scan time 2 min. Scans started after (a, top) 13, (b, middle) 20, and (c, bottom) 27 min.

the centered to the outer regions of the sensor array. After 80 min, the glucose signals effectively reached a "plateau" of around 0.03 mA/cm^2 (not depicted).

The plot surfaces in Figure 11 are quite noisy. This was the result of electronic interferences which disturbed the measurement of the very small individual electrode signals. In Figure 11c, the absolute current values of the array electrodes ranged from approximately 50 pA to 0.5 nA.

CONCLUSIONS

The amperometric imaging of oxygen, hydrogen peroxide, and glucose distributions was realized using an array of 400 individually addressable platinum microelectrodes. The scan time employed in this work was adjusted to 2 min, but in future this may still be reduced. The time-resolved imaging of analyte diffusion was possible with a local resolution of 500 μm. Compared with SECM, this resolution is relatively poor, but in principle, silicon thin-film technology enables structural resolutions of less than 1 μm. Thus, future sensor arrays may realize better local resolutions.

Apart from analyte imaging, the array of individually addressable microelectrodes offers further applications: it may also be used for multianalyte determinations. Therefore, individual microelectrodes will have to be modified by different analyte-specific membranes. In case of a modification by enzyme membranes, this can be carried out very easily and controlled spatially by the method of enzyme immobilization via electrochemical entrapment into the conducting polymer polypyrrole.

Moreover, the sensor array may be used for pattern recognition analysis by using membranes with different sensitivities or selectivities or by applying different working potentials to the individual electrodes of a single chip. In these cases the use of neural networks or fuzzy logic will certainly become very interesting as a powerful tool for data processing.

ACKNOWLEDGMENT

We thank the Bundesministerium für Forschung und Technologie (BMFT, Grant 414-4013-13 MV 0357) and the Ministerium für Wissenschaft und Forschung des Landes Nordrhein-Westfalen for financial support and Dr. Calum Mc Neil from the University of Newcastle upon Tyne (United Kingdom) for a critical discussion of the manuscript.

Received for review November 8, 1994. Accepted January 29, 1995.[⊗]

AC941085N

[⊗] Abstract published in *Advance ACS Abstracts,* March 1, 1995.